

1 A meiotic drive element in the maize pathogen *Fusarium verticillioides* is located within a 102-
2 kb region of chromosome V.

3

4 Jay Pyle*, Tejas Patel*, Brianna Merrill*, Chabu Nsokoshi*, Morgan McCall*, Robert H.
5 Proctor[†], Daren W. Brown^{†,2}, and Thomas M. Hammond^{*,2}

6

7 *School of Biological Sciences, Illinois State University, Normal, IL 61790, and [†]National
8 Center for Agricultural Utilization Research, USDA-ARS, Peoria, IL 61604

9

10 Data deposition: Genome sequencing data are available through NCBI's Sequence Read Archive
11 under accession numbers SRR3271586, SRR3273544, SRR3273545, and SRR3273546. Other
12 sequence data are available from GenBank (KU963213).

13

14 ²Corresponding authors: National Center for Agricultural Utilization Research 1815 N
15 University St., Peoria, IL 61604. E-mail: daren.brown@ars.usda.gov; Illinois State University,
16 School of Biological Sciences, Julian Hall 210, Campus Box 4120, Normal, IL 61790. E-mail:
17 tmhammo@ilstu.edu.

18

19 Running title

20 A meiotic drive element in Fusarium

21

22 **KEYWORDS**

23 genomic conflict, mapping, meiotic drive, fungi, spore killing

24

25 ²Corresponding authors: National Center for Agricultural Utilization Research 1815 N

26 University St., Peoria, IL 61604. E-mail: daren.brown@ars.usda.gov; Illinois State University,

27 School of Biological Sciences, Julian Hall 210, Campus Box 4120, Normal, IL 61790. E-mail:

28 tmhammo@ilstu.edu.

29

30

31 **ABSTRACT**

32 *Fusarium verticillioides* is an agriculturally important fungus because of its association with
33 maize and its propensity to contaminate grain with toxic compounds. Some isolates of the
34 fungus harbor a meiotic drive element known as *Spore killer* (Sk^K) that causes nearly all
35 surviving meiotic progeny from an $Sk^K \times Spore\ killer\text{-susceptible}$ (Sk^S) cross to inherit the Sk^K
36 allele. Sk^K has been mapped to chromosome V but the genetic element responsible for meiotic
37 drive and spore killing has yet to be identified. In this study, we used cleaved amplified
38 polymorphic sequence markers to genotype individual progeny from an $Sk^K \times Sk^S$ mapping
39 population. We also sequenced the genomes of three progeny from the mapping population to
40 determine their single nucleotide polymorphisms. These techniques allowed us to refine the
41 location of Sk^K to a contiguous 102-kb region of chromosome V, herein referred to as the *Sk*
42 locus. Relative to Sk^S genotypes, Sk^K genotypes have one extra gene within this locus for a total
43 of 42 genes. The additional gene in Sk^K genotypes, named *SKL1* for *Spore Killer Locus 1*, is the
44 most highly expressed gene from the *Sk* locus during early stages of sexual development. The *Sk*
45 locus also has three hypervariable regions, the longest of which includes *SKL1*. The possibility
46 that *SKL1*, or another gene from the *Sk* locus, is an essential component of meiotic drive and
47 spore killing is discussed.

48

49 **INTRODUCTION**

50 *Fusarium verticillioides* is an ascomycete fungus that can exhibit both endophytic and
51 pathogenic growth on maize (Bacon and Hinton 1996; White 1998). The fungus is of agriculture
52 concern because of its ability to cause maize ear and stalk rot, and also because it can
53 contaminate maize kernels with a group of mycotoxins known as fumonisins (Marasas 2001;
54 Brown and Proctor 2016). The problems caused by *F. verticillioides* and its mycotoxins were
55 noticed as early as 1970, when the fungus was correlated with an outbreak of Equine
56 Leukoencephalomalacia (ELEM) in South Africa (Kellerman *et al.* 1972). Since then,
57 fumonisins have been confirmed to cause ELEM in horses (Marasas *et al.* 1988; Kellerman *et al.*
58 1990), pulmonary edema in pigs (Harrison *et al.* 1990), and liver cancer in laboratory rats
59 (Gelderblom *et al.* 1988, 1991). Fumonisin-contaminated grain has also been linked to neural
60 tube defects in humans (Missmer *et al.* 2006). Thus, the potential presence of fumonisins, even
61 in apparently healthy grain, makes it necessary to aggressively screen grain for these mycotoxins
62 before it is used in food or feed. Contaminated grain must be destroyed, resulting in crop losses
63 worth millions of dollars per year (Wu, 2007).

64
65 The primary sources of inoculum for endophytic and pathogenic growth of *F.*
66 *verticillioides* on maize are asexual spores, such as macroconidia and microconidia (Munkvold
67 2003). Sexual spores, called ascospores, may also be important to the *F. verticillioides* life cycle
68 (Reynoso *et al.* 2009). Sexual reproduction in this heterothallic fungus begins when the
69 immature fruiting bodies of one strain are fertilized by a strain of opposite mating type (Martin *et*
70 *al.* 2011). Fruiting bodies are called perithecia and meiosis occurs in spore sacs, called asci,
71 within the perithecia. At the start of meiosis, a single diploid nucleus is formed from the haploid

72 genomes of both parents. This diploid nucleus separates into four haploid nuclei through the
73 standard reductional and equational division stages of meiosis, and subsequently, each of these
74 four haploid nuclei undergo a post-meiotic mitosis to form eight nuclei. Each nucleus is then
75 incorporated into a separate ascospore through a process known as ascospore delimitation. A
76 phenotypically normal ascus should thus contain eight ascospores at maturity in *F*.
77 *verticillioides*.

78
79 During normal development, asci break down and ascospores are exuded from perithecia
80 in gelatinous masses. However, it is possible to examine ascospores within intact asci by
81 perithecial dissection. Kathariou and Spieth used this procedure to discover an allele named
82 *Spore killer* (Sk^K). In $Sk^K \times Sk^S$ crosses, where the latter stands for *Spore killer*-susceptible, asci
83 contain four instead of eight ascospores (Kathariou and Spieth 1982). Early stages of ascus
84 development are cytologically-normal in these crosses, but four ascospores degenerate shortly
85 after ascospore delimitation (Raju 1994). The four surviving ascospores are almost always of the
86 Sk^K genotype (Kathariou and Spieth 1982; Xu and Leslie 1996). Unlike $Sk^K \times Sk^S$ crosses, $Sk^K \times$
87 Sk^K crosses produce asci with eight ascospores (Kathariou and Spieth 1982). Thus, the Sk^K allele
88 is sufficient for spore killing and resistance to spore killing.

89
90 The ability of Sk^K -ascospores to kill Sk^S -ascospores suggests that Sk^K could be the
91 predominant allele in some *F. verticillioides* populations. Although the literature is limited on
92 this subject, a screen of 225 *F. verticillioides* isolates from 24 fields across Europe and North
93 America found the Sk^K allele to be present in 81% of isolates (Kathariou and Spieth 1982).
94 Shortly after the discovery of Sk^K in *F. verticillioides*, a spore killing allele was also discovered

95 in *F. subglutinans*. This allele was also named *Spore killer*, but it was given the slightly different
96 notation of SK^k . Along with the report of its discovery, Sidhu (1984) presented evidence that the
97 SK^k allele was present in 10 of 15 *F. subglutinans* isolates obtained from a single maize field.
98 Therefore, Sk^K and SK^k appear to be the predominant alleles in at least some populations of *F.*
99 *verticillioides* and *F. subglutinans*.

100

101 The relationship between Sk^K and SK^k is still unclear despite both being discovered more
102 than 30 years ago. To our knowledge, the only other significant research involving either allele
103 was performed by Xu and Leslie (1996) during construction of a genetic map for *F.*
104 *verticillioides*. During this study, Sk^K was mapped between two restriction fragment length
105 polymorphism (RFLP) markers on chromosome V. These markers, named RFLP1 and 11p18,
106 are located 2.5 cM and 8.6 cM from Sk^K , respectively (Xu and Leslie 1996). Xu and Leslie's
107 mapping population was derived from an $Sk^K \times Sk^S$ cross, and interestingly, only one progeny
108 from over 100 did not inherit the Sk^K allele (Xu and Leslie 1996). This evidence demonstrates
109 that Sk^K can achieve transmission rates of over 99 percent in laboratory crosses.

110

111 An *F. verticillioides* reference genome, derived from an Sk^S strain known as Fv149- Sk^S ,
112 was published 14 years after the initial mapping of Sk^K (Ma *et al.* 2010). Here, we advance
113 *Fusarium* Spore killer research by delineating physical borders for Sk^K with respect to the *F.*
114 *verticillioides* reference genome. Our data place Sk^K within a 102-kb contiguous sequence of
115 DNA, which we refer to as the *Sk* locus. Notable differences exist between the *Sk* locus in
116 Fv999- Sk^K and Fv149- Sk^S strains. These are described and discussed below.

117

118 MATERIAL AND METHODS

119 Strains, media and culture conditions

120 Key strains are listed in Table 1. Vegetative propagation was performed on V8 Juice Agar
121 (VJA) (Tuite, 1969) in 16 mm test tubes at room temperature on a laboratory benchtop. Carrot
122 agar (CA), which was originally described by Klittich and Leslie (1988), was prepared as
123 follows: 200 g of organic peeled baby cut carrots were autoclaved in 200 ml of water, pureed
124 with a blender, then adjusted to 500 ml with sterile water to create a 1× stock. Diluted CA (*e.g.*,
125 0.1× and 0.25×) was prepared by mixing the appropriate volumes of 1× CA stock and sterile
126 water, before adding agar to a final concentration of 2% and autoclaving. Liquid Vogel's
127 Minimal Medium (VMM, Vogel 1956) or GYP medium (2% glucose, 1% peptone, and 0.3%
128 yeast extract) were used to produce mycelia for genomic DNA isolation. Liquid cultures for
129 genomic DNA isolation were incubated at 28 °C in the dark without agitation.

130

131 Sexual crosses

132 Crosses were performed on CA in a similar manner to previously described methods (Klittich
133 and Leslie 1988). Asexual spores (conidia) from the female parent were transferred to the center
134 of a 60 mm petri dish containing 20 ml of CA or diluted CA. The female parent was then
135 cultured for 10-14 days before fertilization with a suspension of conidia from the male parent.
136 Conidial suspensions were prepared by adding 2.0 ml of 0.001% Tween-20 to a 10-14 day old
137 test-tube culture of the male parent and dislodging the conidia with a pipette tip. Fertilization
138 was performed by transferring 1.0 ml of a conidial suspension of the male parent to the surface
139 of a culture of the female parent. The conidial suspension was spread over the surface of the
140 female culture with a glass rod. Crosses were incubated in a culture chamber that alternated

141 between 23.0 °C (12 hours, light) and 22.5 °C (12 hours, dark). Light was provided by white
142 (Philips F34T12/CW/RS/EW/ALTO) and black (General Electric F40T12BL) fluorescent lamps.

143

144 **The Fv999-*Sk*^K × Fv149-*Sk*^S mapping population**

145 In *F. verticillioides*, ascospores are exuded from mature perithecia in a hair-like structure called a
146 cirrus. To obtain an *Sk*^K mapping population, Fv999-*Sk*^K was crossed with Fv149-*Sk*^S and cirri
147 were isolated from the tops of a few perithecia with a sterile needle, dispersed in sterile water,
148 and spread onto a plate of 4% water agar. Germinating ascospores were transferred to VJA in 16
149 mm test tubes.

150

151 **Microscopy**

152 Asci were dissected from perithecia in 25% glycerol under magnification. A Vanguard 1433Phi
153 light microscope and attached digital camera (Amscope MU1000) were used for imaging. The
154 condenser and aperture diaphragm were set for high contrast, which allowed for the number of
155 ascospores in mature asci to be determined without tissue staining.

156

157 **DNA methods**

158 Genomic DNA was prepared using one of three methods. In method one, strains were cultured
159 in 25 ml liquid VMM at 28 °C in the dark for three days. Mycelia were washed with 0.9% NaCl
160 and dried by lyophilization before extraction with IBI Scientific's Genomic DNA Mini Kit for
161 Plants. Method two, based on Henderson *et al.* (2005), was used as an inexpensive and time-
162 efficient alternative to method one. A 6" plain-tipped wood applicator was used to transfer ≤ 10
163 mg of conidia to 200 µl of TE buffer (10 mM Tris, 1 mM EDTA, pH 8.0). The suspension was

164 boiled at 105 °C in a heat block for 12 minutes, incubated on ice for 2 minutes, then vortexed for
165 5 seconds. Insoluble material was pelleted at 15,000 × g for 10 minutes at room temperature,
166 after which 25 µl of supernatant was transferred to a new vial and frozen at -20 °C for storage.
167 In our hands, this method works well for the amplification of PCR products shorter than 1 kb.
168 Method three was used for the preparation of genomic DNA for high-throughput sequencing.
169 Strains were cultured in 25 ml of liquid GYP at 28 °C for 48 hrs. Mycelia was washed with
170 water and DNA was extracted with the Zymo Research Fungal DNA Miniprep Kit.

171

172 Polymerase chain reaction (PCR) assays were performed with MidSci Bullseye Taq DNA
173 Polymerase or New England Biolabs Phusion High-Fidelity DNA Polymerase.

174

175 **Genome sequencing**

176 DNA libraries for MiSeq sequencing (Illumina) were constructed from 1 ng of genomic DNA
177 using the Illumina Nextera XT DNA Library Preparation Kit. Sequencing was performed with
178 MiSeq Reagent Kit Version 3. Adapters were removed and low-quality reads were trimmed with
179 CLC Genomics Workbench (Version 8.0). The datasets were deposited in the National Center
180 for Biotechnology Information's (NCBI) Sequence Read Archive (Leinonen *et al.* 2011). They
181 can be obtained with the following accession numbers: SRR3271586 (Fv999-*Sk^K*), SRR3273544
182 (JP98.75-*Sk^K*), SRR3273545 (JP98.111-*Sk^K*), and SRR3273546 (JP98.118-*Sk^K*). The data sets
183 are of high-quality. For example, draft genomes were assembled with CLC Genomics
184 Workbench and all assemblies had N50 values over 90 kb with coverage levels between 49 and
185 73 fold (Table 2).

186

187 **CAPS markers**

188 Cleaved amplified polymorphic sequence (CAPS) markers (Konieczny and Ausubel 1993) were
189 used to help refine the location of Sk^K (Table 3). CAPS markers were identified by first aligning
190 genome sequencing reads from strain Fv999- Sk^K to the Fv149- Sk^S reference genome (NCBI,
191 ASM14955v1) and then visually scanning aligned reads with Tablet (Milne *et al.* 2010) for
192 polymorphisms in GGCC sites. This four-base sequence is cleaved by the restriction
193 endonuclease *HaeIII*. Six CAPS markers on chromosome V were chosen for this study, along
194 with one CAPS marker on each of chromosomes I, VII, and XI (Table 3). PCR-primers for each
195 CAPS marker were designed to amplify a short product (< 500 bp) from both Fv999- Sk^K and
196 Fv149- Sk^S sequences. The PCR primers used for amplification of each CAPS marker are
197 described in Table S1.

198

199 The following protocol was used to analyze the segregation patterns of CAPS markers in
200 each individual of the Fv999- Sk^K × Fv149- Sk^S mapping population. Genomic DNA was isolated
201 from each progeny, CAPS markers were amplified by PCR, and PCR products were digested
202 with *HaeIII*. The digested products were then examined for Fv999- Sk^K or Fv149- Sk^S cleavage
203 patterns by gel electrophoresis on standard 1% agarose-TAE (40mM Tris, 20mM acetic acid, and
204 1mM EDTA) gels. The *HaeIII*-based DNA digest patterns of each CAPS marker for Fv999- Sk^K
205 and Fv149- Sk^S alleles are listed in Table S2.

206

207

208 **Single nucleotide polymorphisms (SNPs)**

209 Reads from each MiSeq dataset were aligned to the reference genome of strain Fv149-*Sk*^S with
210 Bowtie 2 (Langmead and Salzberg 2012). SAMtools 1.3 and BCFtools 1.3 were then used to
211 report SNPs in variant call format (VCF) (Li *et al.* 2009; Danecek *et al.* 2011). Only reads that
212 matched to a single region of Fv149-*Sk*^S with less than 10 mismatches were used to produce the
213 VCF files. Custom Perl scripts were then used to extract significant SNPs from the VCF files.
214 Significant SNPs were defined as those which were supported by at least 90% of reads at each
215 position. Only positions covered by more than nine reads were considered. Polymorphisms
216 caused by insertions or deletions were ignored.

217

218 **Gene predictions**

219 Protein-coding genes within the *Sk* locus of Fv999-*Sk*^K were predicted as follows: first, the
220 sequence of the *Sk* locus in Fv999-*Sk*^K was obtained by *de novo* assembly of MiSeq reads (Table
221 2); second, the coding sequences of annotated genes from the *Sk* locus of Fv149-*Sk*^S were
222 obtained from GenBank (CM000582.1); third, the Fv149-*Sk*^S coding sequences were aligned to
223 the *Sk* locus of Fv999-*Sk*^K with Clustal Omega (Sievers *et al.* 2011; Li *et al.* 2015); and fourth,
224 the alignments were used to manually annotate protein-coding sequences within the sequence of
225 the Fv999-*Sk*^K *Sk* locus. These steps identified 41 putative protein-coding genes within the *Sk*
226 locus of Fv999-*Sk*^K. Augustus 3.2.1 (Stanke and Waack 2003) was then used for *de novo*
227 prediction of protein-coding genes. Augustus predictions matched our manual annotation with
228 the notable exception of an additional identified gene (*SKL1*, described below) within the *Sk*
229 locus of Fv999-*Sk*^K. The complete sequence and annotation of the 102-kb *Sk*^K locus from Fv999-
230 *Sk*^K can be obtained from GenBank with accession number KU963213.

231

232 **RESULTS**

233 **Increased production of fruiting bodies by strain Fv999-*Sk*^K on diluted CA**

234 Directional crosses are often used to investigate sexual processes in heterothallic ascomycete
235 fungi. In this type of cross, one parent is designated as the female and the other is designated as
236 the male. The female provides protoperithecia, *i.e.*, immature fruiting bodies, which are
237 fertilized by conidia from the male. After fertilization, protoperithecia develop into perithecia.

238 Carrot Agar (CA) is commonly used as a growth medium to study sexual processes in *F.*
239 *verticillioides*. Its preparation essentially involves purchasing carrots from a local market,
240 followed by peeling, blending, and autoclaving a predetermined weight of carrots within a
241 specified volume of water (Leslie and Summerell 2006). Because we were curious about how
242 the amount of carrot in CA medium influences the productivity of Fv999-*Sk*^K × Fv149-*Sk*^S
243 crosses, Fv999-*Sk*^K was cultured on 0.001×, 0.01×, 0.1×, 0.25×, 0.5×, and 1.0× CA, then
244 fertilized with Fv149-*Sk*^S conidia. The crosses performed on 0.1× and 0.25× CA resulted in
245 nearly three to six fold more perithecia than the crosses performed on 0.5× and 1.0× CA (Figure
246 1). No perithecia were produced when crosses were performed on 0.001× and 0.01× CA (Figure
247 1). Additionally, less conidia were produced on 0.1× CA than on 0.25× CA (data not shown).
248 Because conidia can be a source of cross-contamination, 0.1× CA was used as the crossing
249 medium for the remainder of this study.

250

251 **RFLP 11p18 overlaps with *FVEG_02851* on chromosome V**

252 Although the sequence of RFLP1 was not available, we obtained the sequence of RFLP 11p18
253 from the *Fusarium* Comparative Database. We used this sequence as the query in a BLASTn
254 (Altschul *et al.* 1990) search of the *F. verticillioides* reference genome. This search identified

255 positions 1672753 to 1673602 on chromosome V (CM000582.1) as a match to 11p18. This
256 region overlaps with most of the predicted coding sequence of gene *FVEG_02851*, which spans
257 positions 1672886 to 1673769 and encodes a protein of unknown function. Its position on
258 chromosome V was used to choose CAPS markers near the *Sk* locus (Figure 2A).

259

260 **Loci linked to *Sk^K* drive through meiosis**

261 To begin refining the location of *Sk^K* on chromosome V, Fv999-*Sk^K* was crossed with Fv149-*Sk^S*
262 and the segregation patterns of nine CAPS markers were examined in 60 progeny. Both Fv999-
263 *Sk^K* and Fv149-*Sk^S* patterns were inherited in a 1:1 ratio for chromosomes XI, VII, and I. In
264 contrast, Fv999-*Sk^K* patterns of CAPS markers on chromosome V were inherited more frequently
265 ($\geq 79.6\%$) than expected (Figure 2B and Table S3). The only exception was CAPS-5, which is
266 located approximately 20 kb from a telomere (Figure 2A and Table 3). Overall, these results
267 mark the first independent confirmation of Xu and Leslie's (1996) original findings on the biased
268 recovery of molecular markers linked to *Sk^K* in *Sk^K × Sk^S* crosses.

269

270 **Genome sequencing refines the *Sk* locus to a 102-kb region of chromosome V.**

271 To delineate the position of *Sk^K* on chromosome V, we narrowed our focus to progeny JP98.75-
272 *Sk^K*, JP98.111-*Sk^K*, and JP98.118-*Sk^K*. Even though CAPS marker analysis failed to identify an
273 Fv999-*Sk^K* region of chromosome V that was inherited by all three progeny (Figure 2C, black
274 shaded regions), all were determined to carry the *Sk^K* allele by phenotypic analysis (Figure 3 and
275 data not shown). Therefore, their genomes were sequenced (Table 2) and their SNPs along
276 chromosome V were examined. This analysis allowed us to identify two additional
277 recombination events. Both of these recombination events occurred between CAPS markers

278 CAPS-3 and CAPS-4 in the ascus producing progeny JP98.111-*Sk^K* (Figure 2D), explaining why
279 they were not revealed by our CAPS marker analysis. More importantly, the SNP profiles of all
280 three progeny require that *Sk^K* be located between positions 665,669 and 767,411 (Figure 2D, red
281 lines) with respect to the reference sequence (GenBank, CM000582.1). We refer to this 102-kb
282 contiguous sequence as the *Sk* locus (GenBank, KU963213).

283

284 ***Sk^K* strains carry a unique gene in the *Sk* locus**

285 The *Sk* locus spans 102,256 bases in Fv999-*Sk^K*, but only 101,743 bases in Fv149-*Sk^S*. A
286 ClustalW-based alignment (Thompson *et al.* 1994) of the sequences from both strains is 102,557
287 bases long, with 301 gaps in the Fv999-*Sk^K* sequence and 814 gaps in the Fv149-*Sk^S* sequence
288 (Figure 4). To identify specific regions in *Sk^K* and *Sk^S* strains with high levels of SNPs or gaps,
289 the number of SNPs or gaps were calculated for each 100-base window across the alignment. A
290 qualitative analysis of these results finds at least three hypervariable regions (Figure 4). One of
291 the shorter hypervariable regions spans genes *FVEG_03180* to *FVEG_03175*, while another
292 spans genes *FVEG_03174* and *FVEG_03173* (Figure 4). The longest hypervariable region is
293 approximately 14 kb long, spans gene *FVEG_03167*, and extends to the right border of the *Sk*
294 locus (Figure 4).

295

296 The 102-kb *Sk* locus in strain Fv149-*Sk^S* includes 41 putative protein coding genes
297 (Figure 4 and Table 4). The *Sk* locus in Fv999-*Sk^K* carries the same 41 genes as well as one
298 additional protein coding gene, *SKL1* (for *Spore Killer Locus 1*), that is located between
299 *FVEG_03165* and *FVEG_03164* (Figure 4). . BLASTp analysis (Altschul *et al.* 1997) of the
300 NCBI non-redundant protein database with the predicted 70-amino acid sequence of the putative

301 Skl1 protein identified hypothetical proteins with Expect values ranging from 2×10^{-49} to 8×10^{-04}
302 from various *formae speciales* of the *F. oxysporum* species complex. No significant hits were
303 identified in other species (data not shown). A search of the NCBI Conserved Domain Database
304 (Marchler-Bauer *et al.* 2010) failed to identify a domain within Skl1.

305
306 To confirm that *SKLI* is absent in Fv149-*Sk^S*, the sequences corresponding to the
307 *FVEG_03165-FVEG_03164* intergenic region from Fv999-*Sk^K* and Fv149-*Sk^S* were aligned and
308 examined. This intergenic region consists of 1,234 and 755 bases in Fv999-*Sk^K* and Fv149-*Sk^S*
309 respectively (Figure S1). Examination of the alignment revealed that this difference in length
310 was due to the presence of *SKLI* in Fv999-*Sk^K* and its absence in Fv149-*Sk^S* (Figure S1). To
311 confirm that the absence of *SKLI* in Fv149-*Sk^S* was not due to an error in the reference genome
312 sequence, we examined the lengths of the *FVEG_03165-FVEG_03164* intergenic region by PCR
313 in our laboratory stocks of Fv999-*Sk^K* and Fv149-*Sk^S*. The PCR product lengths were consistent
314 with the presence of *SKLI* in Fv999-*Sk^K* and its absence in Fv149-*Sk^S* (Figure 5).

315
316 ClustalW alignments were used to investigate the level of polymorphism between
317 proteins encoded by the *Sk* locus in Fv999-*Sk^K* and Fv149-*Sk^S* strains (Table 4). Analysis of
318 these pairwise alignments revealed that Fveg_15199 is the most polymorphic protein of the
319 locus. Only 80% of the 133 amino acids of Fveg_15199 are identical between the two strains.
320 This is a remarkably high level of polymorphism given that 34 of the 41 shared proteins within
321 the *Sk* locus of Fv999-*Sk^K* and Fv149-*Sk^S* are greater than 94% identical, and 40 of 41 are greater
322 than 88% identical (Table 4). A BLASTp search of the NCBI non-redundant protein database
323 identified homologs of Fveg_15199 in several *Fusarium*, *Neonectria*, *Neosartorya*, and

324 *Aspergillus* species, among others (data not shown). A search of the NCBI Conserved Domain
325 Database failed to identify a domain within Fveg_15199.

326

327 To shed light upon the transcriptional profile of protein-coding genes within the *Sk* locus,
328 we analyzed five *F. verticillioides* RNAseq datasets from NCBI's Sequence Read Archive.
329 These datasets were for five time points following the induction of sexual development in a cross
330 of Fv999-*Sk*^K × Fv149-*Sk*^S (Sikhakolli *et al.* 2012). Of the genes within the *Sk* locus,
331 *FVEG_03171* exhibited the greatest increase in expression from the first to last time point (Table
332 5), suggesting that this gene may have an important role during later stages of sexual
333 development. The corresponding protein, Fveg_03171, includes a WSC-domain (data not
334 shown), which has been linked to carbohydrate-binding, cell wall integrity, and stress response.
335 The gene *FVEG_03194* exhibited the greatest fold change over all five time points (>1050×)
336 (Table 5). The Fveg_03194 protein does not have any recognized domains, although it is
337 conserved in *Fusarium*, *Nectria*, *Trichoderma*, *Colletotrichum*, and a few other fungi (data not
338 shown). Interestingly, *SKLI* reached the highest level of expression of all examined genes 2
339 hours after fertilization (Table 5). Furthermore, *SKLI* transcript levels were second only to
340 *FVEG_03197* at the last time point (144 h, Table 5). The latter gene appears to be widely
341 conserved among bacteria and eukaryotes (data not shown), but a function for it or its homologs
342 is unknown.

343

344 **DISCUSSION**

345 The segregation of alternate alleles into separate gametes during meiosis encourages genetic
346 conflict (Burt and Trivers 2008). Evidence for this is found in meiotic drive, which occurs when
347 an allele is transmitted through meiosis in a biased manner. Meiotic drive elements are found in
348 a diverse range of fungi, where they achieve biased transmission through sexual reproduction by
349 killing meiospores carrying an alternate allele (Turner and Perkins 1979; Kathariou and Spieth
350 1982; Raju 1994; Dalstra *et al.* 2003; Grognet *et al.* 2014). Thus, fungal meiotic drive elements
351 are often referred to as Spore killers. The molecular basis of meiotic drive by most Spore killers
352 is unknown.

353

354 The existence of meiotic drive by spore killing in *Fusarium* was first recognized in 1982.
355 More than three decades later, we still do not understand the molecular mechanism that mediates
356 this process. This is similar to the situation in *Neurospora*, where three distinct spore killers,
357 known as *Sk-1*, *Sk-2*, and *Sk-3*, were identified in 1979 (Turner and Perkins 1979). A
358 breakthrough in *Sk-2* research was recently made by refining the location of an *Sk-2* resistance
359 gene to a 52-kb sequence of DNA (Hammond, Rehard, Harris, *et al.* 2012). This provided the
360 necessary foundation to clone and characterize the *Sk-2* resistance gene (Hammond, Rehard,
361 Xiao, *et al.* 2012), which, in turn, allowed for the isolation of killer-less *Sk-2* mutants (Harvey *et*
362 *al.* 2014). Here, we have taken a similar approach towards identifying the genetic basis for *Sk^K*
363 in *F. verticillioides* by first refining the position of *Sk^K* to a 102-kb region of chromosome V.

364

365 As with previous work on *Sk^K* (Xu and Leslie 1996), we observed a biased transmission
366 of *Sk^K*-linked molecular markers (Figure 2B). This is not unexpected since the driving ability of

367 Sk^K should also affect the transmission of alleles linked to Sk^K . This phenomenon is referred to
368 as genetic hitchhiking (Lyttle 1991). The closer a hitchhiker is to a meiotic driver, the more
369 likely it is to be transmitted to the next generation through the sexual cycle. In our study,
370 patterns of CAPS markers from the parent Fv999- Sk^K were inherited at a higher frequency than
371 could be attributed to chance alone for five of six markers on chromosome V, and the
372 transmission bias generally decreased with increasing distance from the Sk locus (Figure 2B).
373 Surprisingly, CAPS-1 and CAPS-2 demonstrated higher levels of hitchhiking than CAPS-4
374 (Figure 2B), despite the latter being closer to the Sk locus (Figure 2D). One explanation for this
375 could be the existence of a recombination hotspot between CAPS-4 and the Sk locus; however,
376 we do not have additional data to support this hypothesis.

377

378 While a recombination hotspot could explain the unexpected decrease in hitchhiking for
379 CAPS-4, the opposite phenomenon of recombination-suppression is often associated with
380 meiotic drive elements (reviewed by Lyttle 1991). For example, *Neurospora Sk-2* requires
381 specific alleles of at least two genes to mediate drive, a resistance gene called *rsk* and a killer
382 gene called *rfk* (Hammond, Rehard, Xiao, *et al.* 2012; Harvey *et al.* 2014). Each gene is located
383 on a different arm of chromosome III (Harvey *et al.* 2014). For $Sk-2$ to succeed as a meiotic
384 driver, it is imperative that an $Sk-2$ ascospore inherit both *rsk* and *rfk* alleles because loss of *rsk*
385 from $Sk-2$ leads to a self-killing genotype (Hammond, Rehard, Xiao, *et al.* 2012). This helps
386 explain why $Sk-2$ is associated with a 30 cM long “recombination-blocked” region of
387 chromosome III (Campbell and Turner 1987; Harvey *et al.* 2014). By suppressing
388 recombination between *rsk* and *rfk*, $Sk-2$ prevents these critical components of its meiotic drive
389 mechanism from separating during meiosis. With respect to *F. verticillioides Sk^K*, recombination

390 suppression, if it exists at all, does not appear to be a significant phenomenon. For example, our
391 CAPS marker analysis identified twelve recombination events between CAPS-3 and CAPS-4 (n
392 = 59, Table S3), and two recombination events between CAPS-2 and CAPS-3 (n = 59, Table
393 S3). This relatively high number of recombination events near the *Sk* locus argues against an *Sk*-
394 2-like recombination block for *Sk^K*.

395
396 If *F. verticillioides Sk^K* requires multiple genes to function as a meiotic drive element, all
397 should be found within the 102-kb *Sk* locus defined by this study. For example, SNP-profiling of
398 progeny JP98.75-*Sk^K*, JP98.111-*Sk^K*, and JP98.118-*Sk^K* indicated that only this region of
399 chromosome V is common between them and the Fv999-*Sk^k* parent (Figures 2D and Figure 4).
400 Assuming spore killing is mediated by two or more distinct genes within the *Sk* locus, the close
401 proximity of these alleles may negate the requirement for a *Neurospora Sk-2*-like recombination
402 block. Alternatively, meiotic drive and spore killing may be mediated by a single gene. A fungal
403 precedent for this is seen in the *het-s* spore killing mechanism of *Podospora anserina* (Coustou
404 *et al.* 1997; Saupe 2011). This system is controlled by two alternate alleles of a single gene,
405 named *het-s* and *het-S*. The former, *het-s*, encodes the HET-s prion and is the meiotic driver,
406 while the latter, *het-S*, encodes the HET-S protein. Interaction of the HET-s prion with HET-S
407 causes HET-S to relocate to cell membranes, resulting in cell death, presumably through loss of
408 membrane integrity (Seuring *et al.* 2012). The *het-s* ascospores escape cell death because they
409 do not produce the HET-S protein, and thus the *het-s* prion is not toxic to them. This is one
410 example of how meiotic drive and spore killing can be mediated by alternate alleles of a single
411 gene in fungi. Grognet *et al.* (2014) have recently identified *spok1* and *spok2*, two additional

412 spore killing genes in *P. anserina*, both of which appear to be single-gene-based meiotic drive
413 systems.

414

415 In the current study, comparative sequence analysis revealed multiple differences
416 between the 102-kb *Sk* locus from *Sk^K* and *Sk^S* strains of *F. verticillioides*. Presumably, one or
417 more of these differences is the genetic basis for the different *Sk* phenotypes exhibited by the
418 strains. An analysis of SNPs and gaps identified at least three hypervariable regions within the
419 locus (Figure 4). The interspersed nature of these regions is somewhat surprising and suggests
420 that they could be under the influence of different selective pressures than the less variable
421 regions of the *Sk* locus. The most striking difference between the *Sk* locus is the presence the
422 *SKLI* gene in *Sk^K* strains and its absence in *Sk^S* strains. Differences between the hypervariable
423 regions and *SKLI* in *Sk^K* versus *Sk^S* strains raise at least two key questions: 1) are the
424 hypervariable regions and/or *SKLI* responsible for spore killing, and 2) do they correspond to the
425 *Sk^K* allele that was previously defined by phenotypic analysis (Kathariou and Spieth 1982). The
426 high levels of expression of *SKLI* throughout sexual development are consistent with its
427 involvement in sexual reproduction. However, in addition to *SKLI* and the hypervariable
428 regions, there are also numerous less dramatic sequence differences between genes and
429 intergenic regions of the *Sk* locus in *Sk^K* and *Sk^S* strains. The current data does not rule out the
430 possibility that one or more of these differences is responsible for the *Sk^K* and *Sk^S* phenotypes.
431 As a result, our efforts are now focused on targeted deletions of *SKLI* and other regions of the *Sk*
432 locus to determine the genetic basis of the spore killing phenotype in *F. verticillioides*.

433

434

435 **ACKNOWLEDGEMENTS**

436 We thank the Fungal Genetics Stock Center (McCluskey *et al.*, 2010) for some of the strains
437 used in this study and the Broad Institute of Harvard and MIT (www.broad.mit.edu) for access to
438 the *Fusarium* Comparative Database. Dr. John Leslie (Kansas State University) and Dr. Frances
439 Trail (Michigan State University) kindly donated Fv999-*Sk*^K and Fv149-*Sk*^S for this study. Chris
440 McGovern and Nathane Orwig of NCAUR provided much appreciated technical assistance. We
441 thank Dr. Sven Saupe (CNRS - Université de Bordeaux) for sharing his knowledge of the *het-s*
442 spore killing mechanism. TMH was supported by a grant from the Eunice Kennedy Shriver
443 National Institute of Child Health and Human Development of the National Institutes of Health
444 (NICHD, 1R15HD076309-01). Mention of trade names or commercial products in this article is
445 solely for the purpose of providing specific information and does not imply recommendation or
446 endorsement by the US Department of Agriculture. USDA is an equal opportunity provider and
447 employer.

448

449 **LITERATURE CITED**

- 450 Altschul, S.F., W. Gish, W. Miller, E.W. Myers, and D.J. Lipman, 1990 Basic local alignment
451 search tool. *J. Mol. Biol.* 215: 403–410.
- 452 Altschul, S. F., T. L. Madden, A. A. Schäffer, J. Zhang, Z. Zhang *et al.*, 1997 Gapped BLAST
453 and PSI-BLAST: a new generation of protein database search programs. *Nucleic Acids*
454 *Res.* 25: 3389–3402.
- 455 Bacon, C. W., and D. M. Hinton, 1996 Symptomless endophytic colonization of maize by
456 *Fusarium moniliforme*. *Can. J. Bot.* 74: 1195–1202.
- 457 Brown, D. W., and R. H. Proctor, 2016 Insights into natural products biosynthesis from analysis
458 of 490 polyketide synthases from *Fusarium*. *Fungal Genet. Biol.* 89: 37-51.
- 459 Burt, A., and R. Trivers, 2008 *Genes in Conflict: The Biology of Selfish Genetic Elements*.
460 Harvard University Press.
- 461 Campbell, J. L., and B. C. Turner, 1987 Recombination block in the *Spore killer* region of
462 *Neurospora*. *Genome* 29: 129–135.
- 463 Coustou, V., C. Deleu, S. Saupe, and J. Begueret, 1997 The protein product of the *het-s*
464 heterokaryon incompatibility gene of the fungus *Podospora anserina* behaves as a prion
465 analog. *Proc. Natl. Acad. Sci. U. S. A.* 94: 9773–9778.
- 466 Dalstra, H.J.P., K. Swart, A.J.M. Debets, S.J. Saupe, and R.F. Hoekstra, 2003 Sexual
467 transmission of the [Het-S] prion leads to meiotic drive in *Podospora anserina*. *Proc.*
468 *Natl. Acad. Sci. U. S. A.* 100: 6616–6621.
- 469 Danecek, P., A. Auton, G. Abecasis, C.A. Albers, E. Banks *et al.*, 2011 The variant call format
470 and VCFtools. *Bioinformatics* 27: 2156–2158.

- 471 Gelderblom, W. C., K. Jaskiewicz, W. F. Marasas, P. G. Thiel, R. M. Horak *et al.*, 1988
472 Fumonisin--novel mycotoxins with cancer-promoting activity produced by *Fusarium*
473 *moniliforme*. Appl. Environ. Microbiol. 54: 1806–1811.
- 474 Gelderblom, W. C., N. P. Kriek, W. F. Marasas, and P. G. Thiel, 1991 Toxicity and
475 carcinogenicity of the *Fusarium moniliforme* metabolite, fumonisin B1, in rats.
476 Carcinogenesis 12: 1247–1251.
- 477 Grognet, P., H. Lalucque, F. Malagnac, and P. Silar, 2014 Genes that bias Mendelian
478 segregation. PLoS Genet. 10: e1004387.
- 479 Hall, T. A., 1999 BioEdit: a user-friendly biological sequence alignment editor and analysis
480 program for Windows 95/98/NT. Nucleic Acids Symp. Ser. 41: 95–98.
- 481 Hammond, T. M., D. G. Rehard, B. C. Harris, and P. K. T. Shiu, 2012 Fine-scale mapping in
482 *Neurospora crassa* by using genome-wide knockout strains. Mycologia 104: 321–323.
- 483 Hammond, T.M., D.G. Rehard, H. Xiao, and P.K.T. Shiu, 2012 Molecular dissection of the
484 *Neurospora* Spore killer elements. Proc. Natl. Acad. Sci. U. S. A. 109: 12093–12098.
- 485 Harrison, L. R., B. M. Colvin, J. T. Greene, L. E. Newman, and J. R. Cole Jr., 1990 Pulmonary
486 edema and hydrothorax in swine produced by fumonisin B1, a toxic metabolite of
487 *Fusarium moniliforme*. J. Vet. Diagn. Investig. 2: 217–221.
- 488 Harvey, A.M., D.G. Rehard, K.M. Groskreutz, D.R. Kuntz, K.J. Sharp *et al.*, 2014 A critical
489 component of meiotic drive in *Neurospora* is located near a chromosome rearrangement.
490 Genetics 197:1165-1174.
- 491 Henderson, S.T., G.A. Eariss, and D. Catcheside, 2005 Reliable PCR amplification from
492 *Neurospora crassa* genomic DNA obtained from conidia. Fungal Genet. Newsl. 52: 24.

- 493 Kathariou, S., and P.T. Spieth, 1982 Spore Killer Polymorphism in *Fusarium moniliforme*.
494 Genetics 102: 19–24.
- 495 Kellerman, T. S., W. F. Marasas, J. G. Pienaar, and T. W. Naudé, 1972 A mycotoxicosis of
496 equidae caused by *Fusarium moniliforme* sheldon. A preliminary communication.
497 Onderstepoort J. Vet. Res. 39: 205–208.
- 498 Kellerman, T. S., W. F. Marasas, P. G. Thiel, W. C. Gelderblom, M. Cawood *et al.*, 1990
499 Leukoencephalomalacia in two horses induced by oral dosing of fumonisin B1.
500 Onderstepoort J. Vet. Res. 57: 269–275.
- 501 Klittich, C., and J.F. Leslie, 1988 Nitrate reduction mutants of *Fusarium moniliforme*
502 (*Gibberella fujikuroi*). Genetics 118: 417–423.
- 503 Konieczny, A., and F.M. Ausubel, 1993 A procedure for mapping *Arabidopsis* mutations using
504 co-dominant ecotype-specific PCR-based markers. Plant J. 4: 403–410.
- 505 Langmead, B., and S.L. Salzberg, 2012 Fast gapped-read alignment with Bowtie 2. Nat.
506 Methods 9: 357–359.
- 507 Leinonen, R., H. Sugawara, and M. Shumway, 2011 The sequence read archive. Nucleic Acids
508 Res. 39: D19–21.
- 509 Leslie, J.F., and B.A. Summerell, 2006 The *Fusarium* Laboratory Manual. Blackwell
510 Publishing, Ames, Iowa.
- 511 Li, W., A. Cowley, M. Uludag, T. Gur, H. McWilliam *et al.*, 2015 The EMBL-EBI
512 bioinformatics web and programmatic tools framework. Nucleic Acids Res. 43: W580–
513 584.
- 514 Li, H., B. Handsaker, A. Wysoker, T. Fennell, J. Ruan *et al.*, 2009 The Sequence
515 Alignment/Map format and SAMtools. Bioinformatics 25: 2078–2079.

- 516 Lyttle, T. W., 1991 Segregation distorters. *Annu. Rev. Genet.* 25: 511–557.
- 517 Ma, L.J., H.C. van der Does, K.A. Borkovich, J.J. Coleman, M.J. Daboussi *et al.*, 2010
518 Comparative genomics reveals mobile pathogenicity chromosomes in *Fusarium*. *Nature*
519 464: 367–373.
- 520 Marasas, W. F. O., 2001 Discovery and occurrence of the fumonisins: a historical perspective.
521 *Environ. Health Perspect.* 109(Suppl 2): 239-243.
- 522 Marasas, W. F., T. S. Kellerman, W. C. Gelderblom, J. A. Coetzer, P. G. Thiel *et al.*, 1988
523 Leukoencephalomalacia in a horse induced by fumonisin B1 isolated from *Fusarium*
524 *moniliforme*. *Onderstepoort J. Vet. Res.* 55: 197–203.
- 525 Marchler-Bauer, A., S. Lu, J. B. Anderson, F. Chitsaz, M. K. Derbyshire *et al.*, 2010 CDD: a
526 Conserved Domain Database for the functional annotation of proteins. *Nucleic Acids*
527 *Res.* 39: D225–D229.
- 528 Martin, S. H., B. D. Wingfield, M. J. Wingfield, and E. T. Steenkamp, 2011 Structure and
529 evolution of the *Fusarium* mating type locus: new insights from the *Gibberella fujikuroi*
530 complex. *Fungal Genet. Biol.* 48: 731–740.
- 531 McCluskey, K., A. Wiest, M. Plamann, 2010 The Fungal Genetics Stock Center: a repository
532 for 50 years of fungal genetics research. *J. Biosci.* 35: 119–126.
- 533 Milne, I., M. Bayer, L. Cardle, P. Shaw, G. Stephen *et al.*, 2010 Tablet—next generation
534 sequence assembly visualization. *Bioinformatics* 26: 401–402.
- 535 Missmer, S. A., L. Suarez, M. Felkner, E. Wang, A. H. Merrill Jr. *et al.*, 2006 Exposure to
536 fumonisins and the occurrence of neural tube defects along the Texas-Mexico border.
537 *Environ. Health Perspect.* 114: 237–241.

- 538 Mortazavi, A., B. A. Williams, K. McCue, L. Schaeffer, and B. Wold, 2008 Mapping and
539 quantifying mammalian transcriptomes by RNA-Seq. *Nat. Methods* 5: 621–628.
- 540 Munkvold, G. P., 2003 Epidemiology of *Fusarium* diseases and their mycotoxins in maize ears,
541 pp. 705–713 in *Epidemiology of Mycotoxin Producing Fungi*, edited by X. Xu, J. A.
542 Bailey, and B. M. Cooke. Springer Netherlands.
- 543 Raju, N.B., 1994 Ascomycete spore killers: Chromosomal elements that distort genetic ratios
544 among the products of meiosis. *Mycologia* 86: 461-473.
- 545 Reynoso, M. M., S. N. Chulze, K. A. Zeller, A. M. Torres, and J. F. Leslie, 2009 Genetic
546 structure of *Fusarium verticillioides* populations isolated from maize in Argentina. *Eur. J.*
547 *Plant Pathol.* 123: 207–215.
- 548 Saupe, S. J., 2011 The [Het-s] prion of *Podospora anserina* and its role in heterokaryon
549 incompatibility. *Semin. Cell Dev. Biol.* 22: 460–468.
- 550 Seuring, C., J. Greenwald, C. Wasmer, R. Wepf, S. J. Saupe *et al.*, 2012 The mechanism of
551 toxicity in HET-S/HET-s prion incompatibility. *PLoS Biol.* 10: e1001451.
- 552 Sidhu, G. S., 1984 Genetics of *Gibberella fujikuroi* V. *Spore killer* alleles in *G. fujikuroi*. *J.*
553 *Hered.* 75: 237–238.
- 554 Sievers, F., A. Wilm, D. Dineen, T. J. Gibson, K. Karplus *et al.*, 2011 Fast, scalable generation
555 of high-quality protein multiple sequence alignments using Clustal Omega. *Mol. Syst.*
556 *Biol.* 7: 539.
- 557 Sikkakolli, U. R., F. López-Giráldez, N. Li, R. Common, J. P. Townsend *et al.*, 2012
558 Transcriptome analyses during fruiting body formation in *Fusarium graminearum* and
559 *Fusarium verticillioides* reflect species life history and ecology. *Fungal Genet. Biol.* 49:
560 663–673.

- 561 Stanke, M., and S. Waack, 2003 Gene prediction with a hidden Markov model and a new intron
562 submodel. *Bioinformatics* 19(Suppl 2): 215–225.
- 563 Thompson, J. D., D. G. Higgins, and T. J. Gibson, 1994 CLUSTAL W: improving the
564 sensitivity of progressive multiple sequence alignment through sequence weighting,
565 position-specific gap penalties and weight matrix choice. *Nucleic Acids Res.* 22: 4673–
566 4680.
- 567 Tuite, J., 1969. *Plant Pathological Methods: Fungi and Bacteria*. Burgess Publishing Company,
568 Minneapolis.
- 569 Turner, B.C., and D.D. Perkins, 1979 *Spore killer*, a chromosomal factor in *Neurospora* that
570 kills meiotic products not containing it. *Genetics* 93: 587–606.
- 571 Vogel, H.J., 1956 A convenient growth medium for *Neurospora* (Medium N). *Microb. Genet*
572 *Bull* 13: 42–43.
- 573 White, D. G. 1998 *Compendium of corn diseases*. APS Press, St. Paul, Minn.
- 574 Wu, F. 2007 Measuring the economic impacts of *Fusarium* toxins in animal feeds. *Animal Feed*
575 *Sci. Technol.* 137: 363-374.
- 576 Xu, J.R., and J.F. Leslie, 1996 A genetic map of *Gibberella fujikuroi* mating population A
577 (*Fusarium moniliforme*). *Genetics* 143: 175–189.
- 578 Xu J.R., K. Yan, M. B. Dickman, and J. F. Leslie, 1995 Electrophoretic karyotypes distinguish
579 the biological species of *Gibberella fujikuroi* (*Fusarium* Section *Liseola*). *Mol. Plant.*
580 *Microbe Interact.* 8: 74–84.
- 581

582 **Figure and Table Legends**

583 **Figure 1** Perithecial production on different CA media. Cultures of Fv999-*Sk^K* were grown on
584 CA media containing different concentrations of carrot and fertilized with conidia from strain
585 Fv149-*Sk^S*. The data represent the total number of perithecia observed 25 days after fertilization.
586 Crosses were performed in triplicate and error bars are standard deviation.

587
588 **Figure 2** The *F. verticillioides Sk* locus is found within a 102-kb region of chromosome V. A)
589 A diagram of the 4.25 Mb sequence of chromosome V from Fv149-*Sk^S* is shown. The annotated
590 chromosome V sequence was downloaded from NCBI (CM000582.1). The first gene
591 (*FVEG_03430*) and last gene (*FVEG_16592*) on the chromosome are indicated. The location of
592 RFLP marker 11p18 is also shown. Marker 11p18 overlaps gene *FVEG_02851*. B) A total of 60
593 progeny were isolated from a cross between Fv999-*Sk^K* and Fv149-*Sk^S*. These progeny were
594 genotyped with nine different CAPS markers. Markers CAPS-1 through CAPS-6 are located on
595 chromosome V. Markers CAPS-9, CAPS-10, and CAPS-11 are found on chromosomes XI, VII,
596 and I, respectively. Each bar represents the percentage of Fv999-*Sk^K* genotypes recovered for
597 each marker. An asterisk is placed above all markers whose recovery deviated significantly from
598 a Mendelian ratio of 1:1 according to a χ^2 test with $p < 0.01$. The biased transmission of Fv999-
599 *Sk^K* sequences was detected for all markers on chromosome V, except for CAPS-5. (C) The
600 marker patterns for progeny JP98.75-*Sk^K*, JP98.111-*Sk^K*, and JP98.118-*Sk^K* suggest that crossover
601 events occurred between CAPS-3 and CAPS-4 (for JP98.75-*Sk^K*), CAPS-4 and CAPS-5 (for
602 JP98.111-*Sk^K*), and CAPS-2 and CAPS-3 (for JP98.118-*Sk^K*) (Table S3). These crossovers do
603 not reveal an Fv999-*Sk^K*-derived chromosome V sequence common to all three progeny. The
604 predicted Fv999-*Sk^K*- and Fv149-*Sk^S*-inherited regions are shown in black and white,

605 respectively. Irregular borders are used to indicate that the exact crossover positions cannot be
606 determined from the marker data. (D) SNP analysis was used to more accurately define
607 crossover positions for progeny JP98.75- Sk^K , JP98.111- Sk^K , and JP98.118- Sk^K , and to discover
608 additional crossovers. This analysis identified two additional recombination events on
609 chromosome V of JP98.111- Sk^K , which delineate a single contiguous region between 665.7 kb
610 and 767.4 kb on chromosome V as the only Fv999- Sk^K region common to all three progeny (red
611 dotted lines). This region is referred to as the *Sk* locus.

612

613 **Figure 3** Representative images of killing and no-killing in *F. verticillioides* asci. (A) Asci
614 from a cross of progeny JP98.111- Sk^K with BM43.31- Sk^K . Eight ascospores can be detected in
615 most of the mature asci, confirming that progeny JP98.111- Sk^K carries the Sk^K allele. (B) Asci
616 from a cross of progeny JP98.111- Sk^K with Fv149- Sk^S . Only four ascospores are detected in
617 most of the mature asci, again confirming that progeny JP98.111- Sk^K carries the Sk^K allele. The
618 asterisk denotes an ascus where there appears to be five ascospores. Two possible explanations
619 are that this 5th ascospore escaped killing, or, it strayed from another ascus during the dissection
620 and imaging process.

621

622 **Figure 4** Strain Fv999- Sk^K carries a unique gene within a hypervariable region of the *Sk* locus.
623 The *Sk* locus from Fv999- Sk^K (GenBank, KU963213) and Fv149- Sk^S (GenBank, CM000582.1,
624 positions 665,669 to 767,411) were imported into BioEdit (Version 7.2.5) (Hall 1999) and
625 aligned with ClustalW. Custom Perl scripts were used to examine base mismatches, gap
626 positions, and to generate the diagram. The total number of mismatches (SNPs) between the two
627 sequences was calculated for each 100-base, non-overlapping window of the alignment. The

628 total number of gaps was also calculated for each 100-base, non-overlapping window. A gap
629 position was not considered an SNP. By this definition, a window with 100 gaps can have no
630 SNPs. Black rectangles represent the coding regions of predicted genes. Gene names are
631 abbreviated according to their identification tags in the Fv149-*Sk^S* annotation. For example:
632 *FVEG_03199* is shortened to *3199*. A striking feature of the alignment is the presence of at least
633 three hypervariable regions; approximately spanning *FVEG_03180* to *FVEG_03175*,
634 *FVEG_3174* to *FVEG_3173*, and *FVEG_03167* to the right border. A second striking feature is
635 the presence of a unique gene, *SKLI*, in Fv999-*Sk^K* only.

636

637 **Figure 5** The *Sk* locus in Fv149-*Sk^S* is missing *SKLI*. To confirm that *SKLI* is missing from the
638 *Sk* locus in Fv149-*Sk^S*, genomic DNA was isolated from two liquid cultures of Fv149-*Sk^S* and
639 two liquid cultures of Fv999-*Sk^K*. All four genomic DNA samples were used as templates in
640 standard PCR reactions with the following oligonucleotide primers: 5'
641 CGAATGACCTGGGGAGCCATAA 3' and 5' TCTCTCCACCACCTCCATCAGC 3', which
642 amplify the *FVEG_03165-FVEG_03164* intergenic regions in Fv999-*Sk^K* and Fv149-*Sk^S*. PCR
643 products were visualized by ethidium bromide staining after electrophoresis through a 1%
644 agarose-TAE gel. We observed PCR products with lengths that are consistent with the absence
645 of *SKLI* in Fv149-*Sk^S* (287 bp) and the presence of *SKLI* in Fv999-*Sk^K* (767 bp).

646

647 **Figure S1** A ClustalW alignment of the *FVEG_03165-FVEG_03164* intergenic region from
648 Fv999-*Sk^K* and Fv149-*Sk^S*. The coding start site of flanking gene *FVEG_03165* is indicated with
649 a blue arrow. Similarly, the coding stop site of flanking gene *FVEG_03164* is indicated with a

650 blue line. The predicted coding sequence of *SKLI* is indicated with a red line. This alignment
651 shows that *SKLI* is present in Fv999-*Sk^K* but not in Fv149-*Sk^S*.

652

653 **Table 1 Key strains used in this study**

654 ¹Throughout the text, the suffix -*Sk^K* or -*Sk^S* is added to each strain name to denote genotype with
655 respect to *Sk*. ²McCluskey *et al.* 2010; ³Xu *et al.* 1995; ⁴Xu and Leslie 1996.

656

657 **Table 2 Draft genome assembly statistics**

658 ¹total, the total length of each genome assembly; ²avg. length, the average length of each read in
659 the assembly; ³coverage, calculated by multiplying the number of reads by the average read
660 length and dividing the product by 41.9 Mb, the genome size of Fv149-*Sk^S* (NCBI
661 ASM14955v1).

662

663 **Table 3 Marker locations**

664 Marker locations on chromosomes I, V, VII, and XI of *F. verticillioides* Fv149-*Sk^S* (NCBI
665 ASM14955v1).

666

667

668

669

670

671

672

673

674 **Table 4 Comparison of predicted protein-coding sequences within the *Sk* locus of Fv999-**

675 ***Sk^k* and Fv149-*Sk^S***

676 The sequences of predicted proteins within the *Sk* locus of Fv999-*Sk^K* and Fv149-*Sk^S* were
677 imported into Bioedit 7.2.5 (Hall 1999) and aligned with ClustalW (Thompson *et al.* 1994).
678 Sequence alignments were then analyzed for percent identity and percent similarity. Gapped-
679 positions were excluded from the identity and similarity calculations.

680

681 **Table 5 Expression analysis of genes from the *Sk* locus during sexual development**

682 Sikkhakolli *et al.* (2012) analyzed transcriptional changes in *F. verticillioides* during fruiting body
683 development in Fv999-*Sk^K* × Fv149-*Sk^S* crosses by RNA sequencing (RNAseq) and deposited the
684 datasets in NCBI's Sequence Read Archive (Leinonen *et al.* 2011). The following datasets were
685 downloaded from the database: 2 hours post fertilization (hpf) (SRR1592416), 24 hpf
686 (SRR1592417), 48 hpf (SRR1592418), 72 hpf (SRR1592419), 96 hpf (SRR1592420), and 144
687 hpf (SRR1592421). Reads were aligned to coding sequences for the 42 genes (plus flanking
688 genes *FVEG_03199* and *FVEG_03163*) from the *Sk* locus in Fv999-*Sk^K* with Bowtie 2
689 (Langmead and Salzberg 2012). RPKK values, or, reads per kilobase exon model per thousand
690 mapped reads, were calculated for each gene. We then performed the same alignment and RPKK
691 calculation procedure for the coding sequences of the 41 genes from the *Sk* locus (plus flanking
692 genes *FVEG_03199* and *FVEG_03163*) in Fv149-*Sk^S*. The RPKK values in the table are the
693 average of the two RPKK calculations for each gene, except for *SKLI*, which is only found in
694 Fv999-*Sk^K*. RPKK is a variation upon RPKM as described by (Mortazavi *et al.* 2008). ¹The
695 minimum RPKK in the table. ²The maximum RPKK in the table. ³Fold change was calculated by

696 dividing the maximum RPKK by the minimum RPKK to identify the genes undergoing the
697 greatest expression change during the first 144 hours after fertilization. If the minimum RPKK
698 for a gene was 0, it was arbitrarily assigned a minimum RPKK of 0.1 to approximate a fold
699 change value.

700

701

702 **Table S1 Oligonucleotide primers for CAPS markers**

703

704 **Table S2 CAPS marker sizes**

705

706 **Table S3 Genotypes of the Fv999-*Sk*^K × Fv149-*Sk*^S mapping population**

707

708

Figure 1

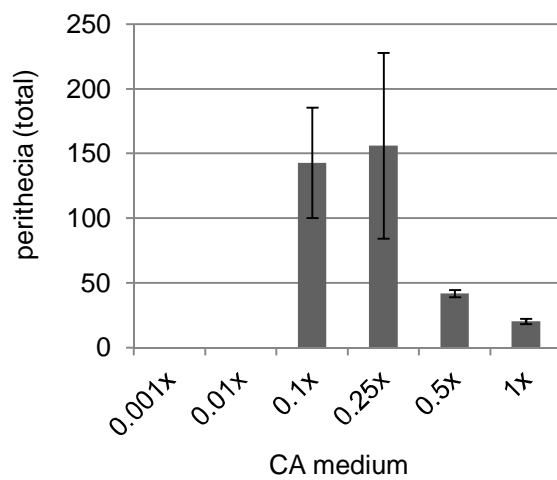


Figure 2

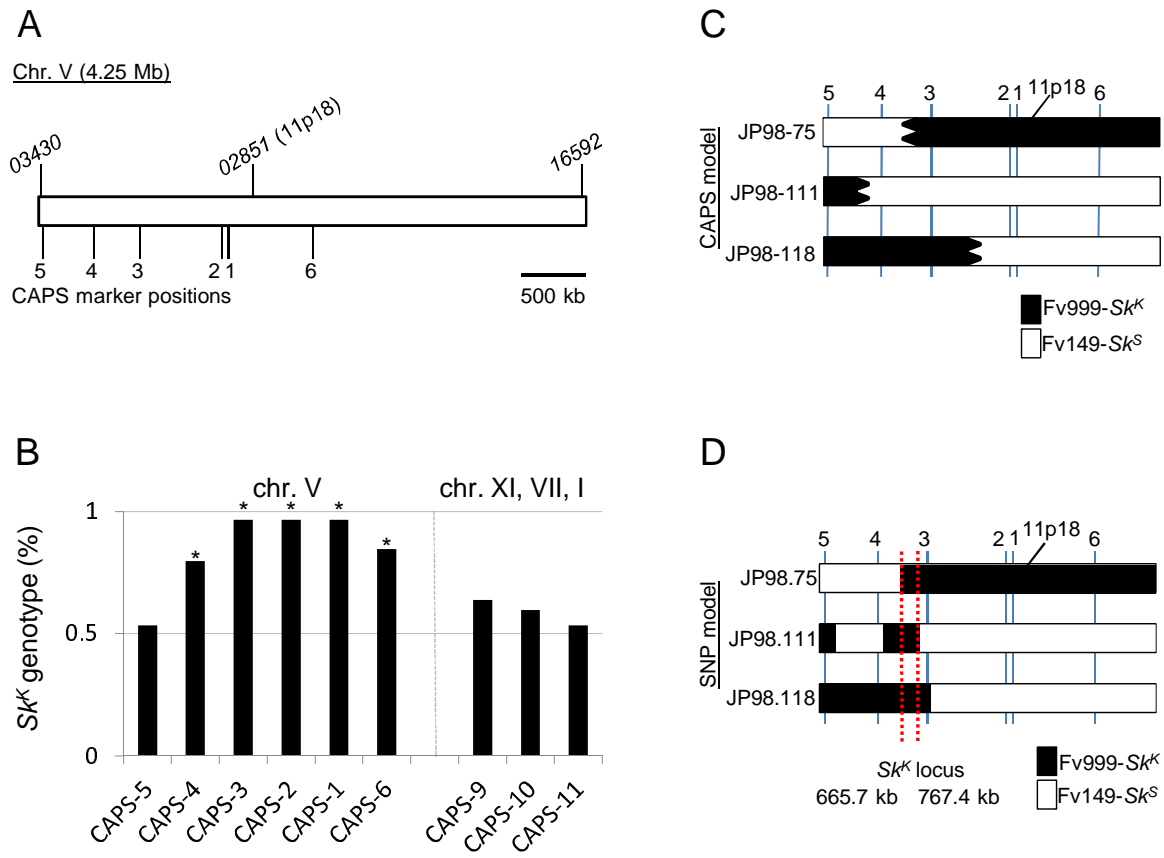


Figure 3

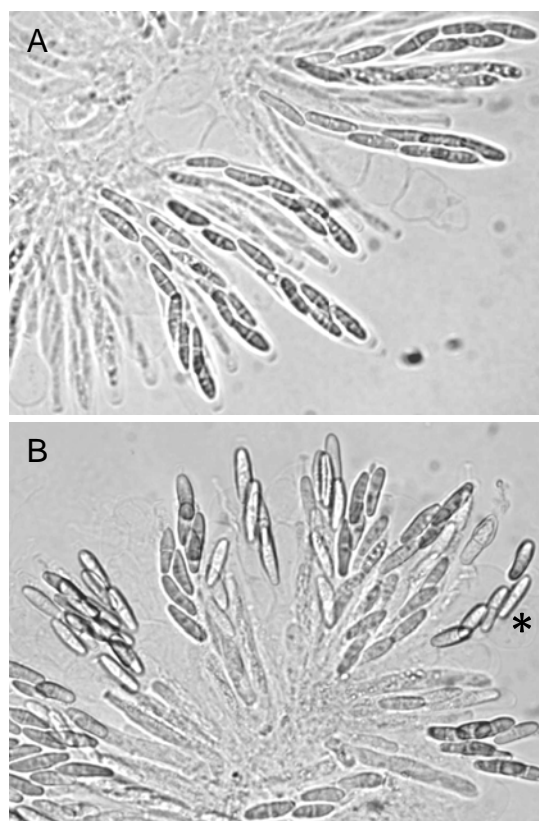
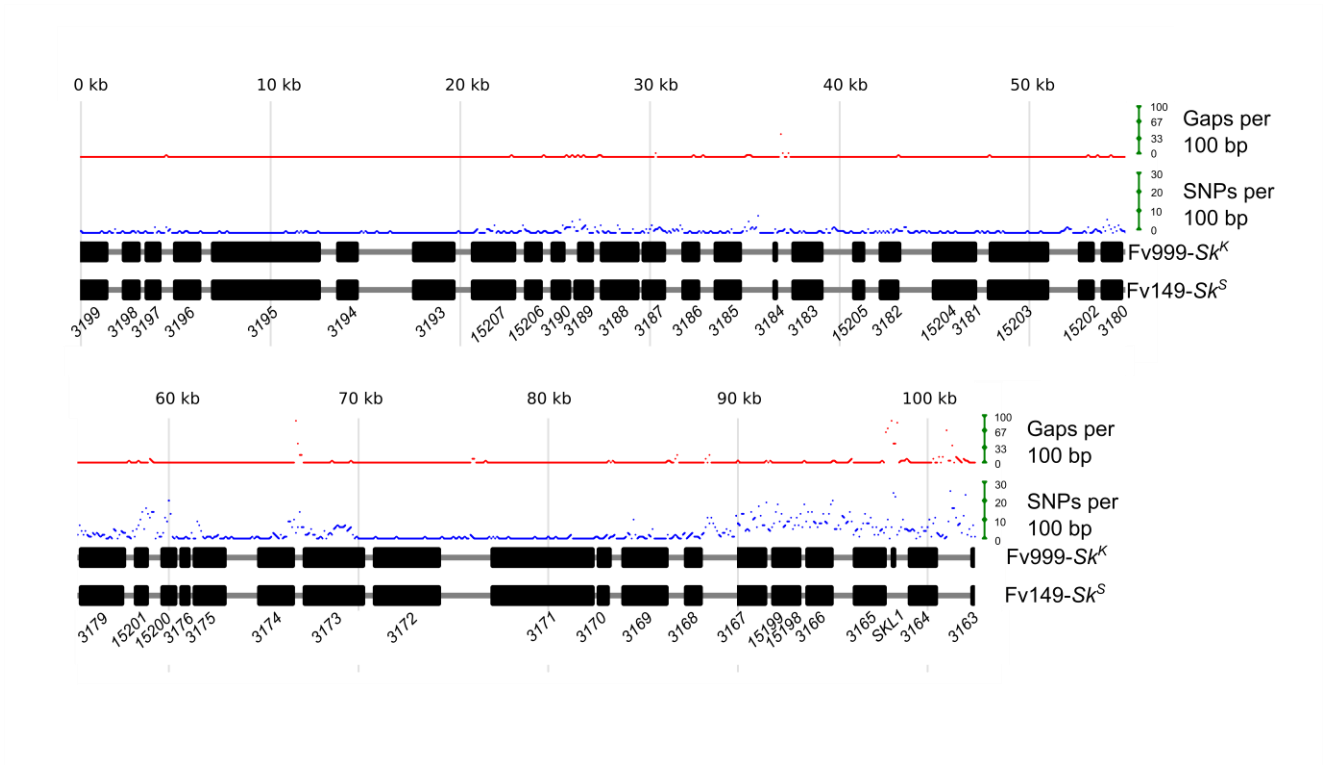


Figure 4



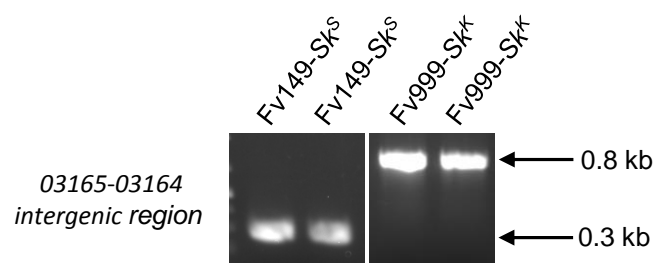


Table 1 Key strains used in this study

name ¹	genotype	alternate names
Fv149	<i>Sk^S</i> , <i>MAT-1</i>	FGSC 7600 ² , M-3125 ³ , A00149 ³
Fv999	<i>Sk^K</i> , <i>MAT-2</i>	FGSC 7603 ² , A00999 ⁴
RJP98.75	<i>Sk^K</i> , <i>MAT-2</i>	this study
RJP98.111	<i>Sk^K</i> , <i>MAT-2</i>	this study
RJP98.118	<i>Sk^K</i> , <i>MAT-2</i>	this study
RBM43.31	<i>Sk^K</i> , <i>MAT-1</i>	this study

Table 2 Draft genome assembly statistics

name	total ¹	contigs	avg. length ²	# reads	N50	coverage ³
Fv999- <i>Sk^K</i>	41,922,529	855	255	10,956,620	109,413	67
RPJ98.75- <i>Sk^K</i>	41,848,894	985	257	8,087,199	91,461	50
RPJ98.111- <i>Sk^K</i>	41,892,017	841	242	12,538,869	120,565	72
RPJ98.118- <i>Sk^K</i>	41,868,129	914	268	9,009,572	88,867	58

Table 3 Marker locations

marker	chromosome	position (Mb)
CAPS-1	V	1.47
CAPS-2	V	1.42
CAPS-3	V	0.78
CAPS-4	V	0.43
CAPS-5	V	0.02
CAPS-6	V	2.12
CAPS-9	XI	0.07
CAPS-10	VII	1.05
CAPS-11	I	0.73
RFLP-11p18	V	1.67

Table 4 Comparison of predicted protein-coding sequences within the *Sk* locus of Fv999-*Sk*^k and Fv149-*Sk*^s

name	Fv999- <i>Sk</i> ^K length	Fv149- <i>Sk</i> ^S length	alignment length	identity (%)	similarity (%)
3198	279	279	279	0.99	0.99
3197	224	224	224	0.99	0.99
3196	462	462	462	1.00	1.00
3195	1786	1786	1786	1.00	1.00
3194	359	359	359	1.00	1.00
3193	655	655	655	1.00	1.00
15207	634	666	692	0.93	0.94
15206	274	274	274	1.00	1.00
3190	146	242	242	0.99	1.00
3189	246	336	336	0.89	0.91
3188	599	599	599	0.99	1.00
3187	327	327	327	0.98	0.99
3186	234	234	234	1.00	1.00
3185	409	409	409	1.00	1.00
3184	65	46	65	0.96	0.98
3183	513	513	513	1.00	1.00
15205	174	174	174	0.99	1.00
3182	379	355	379	0.97	0.98
15204	88	88	88	1.00	1.00
3181	667	667	667	1.00	1.00
15203	1029	1085	1085	0.99	0.99
15202	194	194	194	1.00	1.00
3180	359	359	359	0.97	0.99
3179	784	736	784	0.97	0.97
15201	227	227	227	0.89	0.90
15200	288	288	288	0.93	0.98
3176	139	139	139	1.00	1.00
3175	496	496	496	0.99	1.00
3174	620	620	620	0.96	0.97
3173	964	964	964	0.97	0.98
3172	1018	1018	1018	1.00	1.00
3171	1724	1724	1724	1.00	1.00
3170	230	212	230	0.98	0.98
3169	716	716	716	0.99	0.99
3168	299	299	299	1.00	1.00
3167	460	460	460	0.97	0.98
15199	133	133	133	0.80	0.86
15198	323	319	323	0.93	0.95
3166	466	466	466	0.90	0.95
3165	532	531	532	0.98	0.99
SKL1	70	missing	na	na	na
3164	476	479	479	0.98	0.99

Table 5 Expression analysis of genes from the *Sk* locus during sexual development

ID	2 h	24 h	48 h	72 h	96 h	144 h	Min ¹	Max ²	Fold change ³
3198	39.17	150.92	38.40	24.98	28.10	20.10	20.10	150.92	7.51
3197	256.38	368.62	217.04	122.34	103.97	231.66	103.97	368.62	3.55
3196	0.83	0.13	0.87	0.56	0.83	0.87	0.13	0.87	6.59
3195	2.49	0.57	2.48	0.62	5.80	0.79	0.57	5.80	10.12
3194	0.25	0.12	0.30	14.02	124.53	1.20	0.12	124.53	1050.12
3193	138.42	94.82	71.69	43.35	80.19	75.41	43.35	138.42	3.19
15207	1.41	1.35	16.98	1.71	2.05	2.46	1.35	16.98	12.55
15206	0.78	1.40	5.23	1.29	0.76	1.08	0.76	5.23	6.86
3190	0.00	0.00	0.00	0.00	0.23	0.00	0.00	0.23	2.32
3189	0.00	0.00	0.00	0.05	0.50	0.00	0.00	0.50	4.95
3188	1.73	0.36	1.58	0.48	2.72	0.40	0.36	2.72	7.65
3187	1.90	0.97	1.34	31.36	42.16	0.71	0.71	42.16	59.47
3186	1.45	0.55	0.81	0.77	0.37	0.61	0.37	1.45	3.91
3185	5.41	3.74	6.17	2.61	1.72	1.51	1.51	6.17	4.09
3184	0.58	0.00	1.19	0.84	9.94	0.79	0.00	9.94	99.38
3183	59.62	22.63	32.99	13.12	29.15	21.10	13.12	59.62	4.54
15205	4.06	1.68	6.07	3.12	10.00	1.23	1.23	10.00	8.15
3182	0.30	0.00	1.19	0.00	0.29	0.00	0.00	1.19	11.93
15204	5.10	3.36	84.28	5.20	12.73	5.45	3.36	84.28	25.10
3181	2.16	0.50	5.24	0.50	1.93	0.66	0.50	5.24	10.57
15203	4.74	0.12	3.02	1.00	4.72	0.95	0.12	4.74	39.22
15202	1.05	0.44	8.61	7.61	9.45	0.74	0.44	9.45	21.57
3180	2.20	0.00	3.14	0.14	0.98	0.17	0.00	3.14	31.38
3179	1.28	0.06	1.14	0.10	2.70	0.09	0.06	2.70	47.85
15201	4.11	0.57	4.26	1.33	4.46	0.49	0.49	4.46	9.01
15200	1.02	0.55	0.32	0.36	0.29	0.24	0.24	1.02	4.16
3176	126.00	50.26	80.75	15.66	31.67	29.31	15.66	126.00	8.05
3175	48.87	12.93	38.03	9.13	19.60	13.41	9.13	48.87	5.35
3174	4.53	1.43	8.61	0.94	4.68	1.29	0.94	8.61	9.18
3173	1.04	0.17	2.86	0.42	1.90	0.42	0.17	2.86	17.29
3172	1.01	0.00	3.78	0.45	2.16	0.70	0.00	3.78	37.81
3171	2.95	37.34	38.55	117.07	44.37	94.58	2.95	117.07	39.66
3170	0.14	0.19	0.00	0.81	0.13	0.44	0.00	0.81	8.09
3169	5.48	0.61	5.38	3.02	7.40	2.61	0.61	7.40	12.05
3168	4.33	21.39	2.58	13.90	7.76	2.19	2.19	21.39	9.77
3167	0.17	0.71	0.13	0.21	0.12	0.04	0.04	0.71	19.47
15199	0.07	0.00	0.00	0.00	0.00	0.00	0.00	0.07	0.71
15198	1.34	0.12	0.56	0.21	0.31	0.19	0.12	1.34	11.68
3166	0.99	0.17	1.43	0.24	0.31	0.22	0.17	1.43	8.36
3165	20.77	11.51	13.49	9.68	8.41	4.09	4.09	20.77	5.07
SKL1	481.58	392.59	227.42	211.66	360.52	97.65	97.65	481.58	4.93
3164	16.11	30.78	16.09	6.78	16.48	15.70	6.78	30.78	4.54

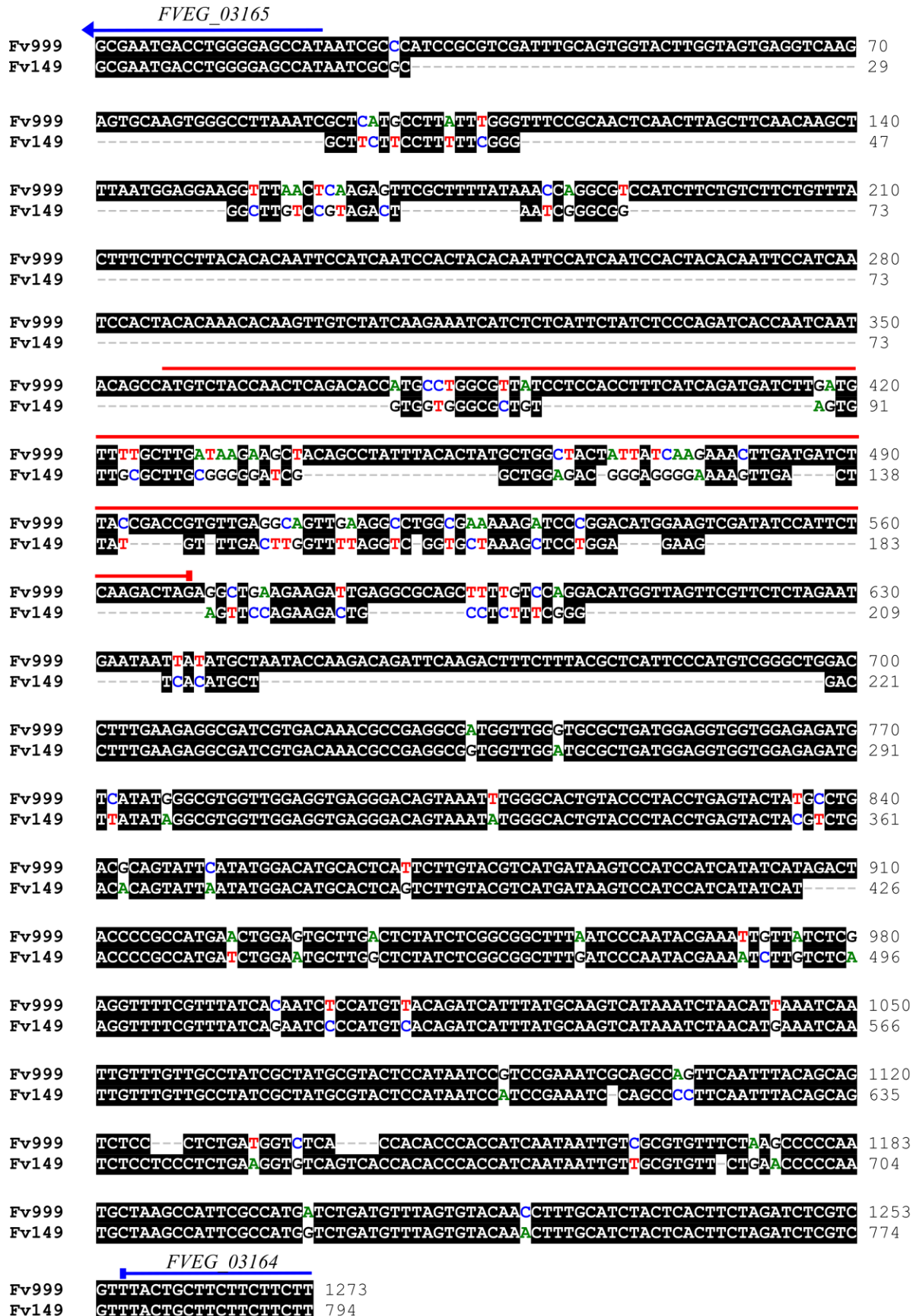


Table S1 Oligonucleotide primers for CAPS markers

Name	Sequence (5' to 3')
CAPS-1F	GCGATACAGAACCCCCATTCTCTT
CAPS-1R	GATCAGCCATCCTATCTCTCCCAGT
CAPS-2F	TTATCTGCACACCTGGAGGA
CAPS-2R	CGGCTTCACCTGAGACATTT
CAPS-3F	CCAGAATGGCTCTGACCTGGTGT
CAPS-3R	GCGCAGATCATGGAGAGGGTATG
CAPS-4F	ATGTGTGCAGCTCGTTTTTG
CAPS-4R	TCAACCCCGAGACTTTCATC
CAPS-5F	GACCAGACCCGAAACCAAT
CAPS-5R	CAGCCAAATCACGCTGTCT
CAPS-6F	GGTCGAGAACAAAGGGGTTC
CAPS-6R	CAAAGATGGGAGGAACATGG
CAPS-9F	CGCGGTTGACACGGCTCTC
CAPS-9R	GAAATGCGGCTCCAATTCTCG
CAPS-10F	TGCTGCCTCGATTCTTCTTCC
CAPS-10R	CGGAGTACCATTGTTTCGGGTGA
CAPS-11F	TGCACAGAAGCGAGACAAACATCC
CAPS-11R	TCGAGCATGACCAAGGCAGAAC

Table S2 CAPS marker sizes

marker	PCR product length	Fv149 product lengths after <i>Hae</i> III digest	Fv999 product lengths after <i>Hae</i> III digest
CAPS-1	358	44, 86, 228,	151, 207
CAPS-2	307	132, 175	307
CAPS-3	311	311	105, 206
CAPS-4	288	110, 178	288
CAPS-5	265	119, 146	265
CAPS-6	325	34, 92, 199	34, 291
CAPS-9	291	128, 163	291
CAPS-10	404	404	68, 336
CAPS-11	333	333	108, 225

#91	K	K	K	K	K	K	K	K	K
#92	S	K	K	K	K	K	K	nd	K
#93	S	K	K	K	K	K	K	K	K
#94	S	K	K	K	K	S	K	K	S
#95	K	K	K	K	K	K	K	K	S
#96	K	K	K	K	K	K	S	K	S
#97	K	K	K	K	K	S	K	K	S
#98	K	K	K	nd	K	K	K	K	K
#99	K	K	K	K	K	K	K	S	S
#100	S	K	K	K	K	K	K	K	S
#101	S	S	K	K	K	K	K	S	K
#102	K	K	nd	K	K	K	S	K	K
#103	K	K	K	K	K	K	S	K	K
#104	S	K	K	K	K	S	S	S	S
#105	S	K	K	K	K	S	K	K	S
#106	S	S	K	K	K	S	S	S	S
#107	K	K	S	K	K	K	S	S	S
#108	K	S	K	K	K	K	K	nd	K
#109	K	K	K	K	K	K	K	K	S
#110	S	S	K	K	K	S	S	S	K
#111	K	S	S	S	S	S	K	S	K
#112	K	K	K	K	K	K	S	nd	K
#113	K	K	K	K	K	K	K	S	S
#114	K	K	K	K	K	K	K	S	S
#115	K	K	K	K	K	nd	S	S	K
#116	S	S	K	K	K	K	K	K	K
#117	K	K	K	K	K	K	K	S	K
#118	K	K	K	S	S	S	K	K	K
#119	S	S	K	K	K	K	K	S	K

The chromosome V CAPS markers (1 through 6) are arranged in the table according to their relative order on the chromosome. K = Fv999-*Sk^K* genotype; S = Fv149-*Sk^S* genotype; nd = not determined.